Polymer Journal (2018) 50:799–804
https://doi.org/10.1038/s41428-018-0057-3

NOTE

Nanoribbon network formation of enzymatically synthesized cellulose oligomers through dispersion stabilization of precursor particles

Takeshi Serizawa[1] · Yuka Fukaya[1] · Toshiki Sawada[1,2]

Received: 19 January 2018 / Revised: 26 March 2018 / Accepted: 31 March 2018 / Published online: 7 May 2018

Introduction

Naturally derived crystalline nanocelluloses with flexible fiber or rigid rod nanostructures have gained considerable attention as naturally abundant and renewable nanomaterials [1–3]. Nanocelluloses are categorized into the three classes: nanofibrillated cellulose, nanocrystalline cellulose, and bacterial nanocellulose [4–6]. The first two nanocelluloses are produced via top-down processes, including mechanical and/or chemical treatments of natural sources, and the third type of nanocellulose is produced by bacteria in culture media using bottom-up processes. Due to the advantageous physicochemical properties of nanocelluloses, such as their chemical/thermal stabilities, mechanical stiffness, lightness, and biocompatibility, diverse potential applications of the nanocelluloses have been investigated for development of novel functional materials [1–3].

Alternatively, enzyme-catalyzed polymerization/oligomerization reactions using cellulase, cellodextrin phosphorylase (CDP), or β-glucan synthetase are utilized for the in vitro synthesis of cellulose molecules via bottom-up processes followed by crystallization-driven self-assembly of the molecules into artificial nanocelluloses with high purity and unique morphologies different from those of natural nanocelluloses [7–10]. For example, when α-D-glucose-1-phosphate (αG1P) monomers (that is, glucosyl donors) are oligomerized from D-glucose (Glc) primers (that is, glucosyl acceptors) in aqueous buffer solutions based on CDP-catalyzed reverse phosphorolysis reactions, two-dimensional rectangular nanosheets composed of cellulose oligomers with degree-of-polymerization (DP) values of 9-10 are produced as precipitates under adequate conditions (Fig. 1a) [11, 12]. Although it is generally difficult to control the product morphologies in precipitation reactions, our previous studies demonstrated the formation of highly grown nanoribbon network structures composed of cellulose oligomers based on the two different strategies for CDP-catalyzed reactions, thereby producing unique cellulosic hydrogels [13–16]. One strategy is based on dispersion stabilization of precursor particles under macromolecular crowding conditions for promotion of crystal growth [13–15]. The other strategy is based on kinetic control of the amounts of the water-insoluble product, where sufficient water-insoluble products for nanoribbon network formation were kinetically produced using adequate primers (i.e., cellobiose) instead of Glc [16]. Consequently, the CDP-catalyzed reactions possess the potential to elicit the self-assembly capability of cellulose oligomers.

In this study, we demonstrate nanoribbon network formation of cellulose oligomers synthesized by CDP-catalyzed reactions using αG1P monomers and Glc primers at relatively high primer concentrations through crystallization-driven in situ self-assembly in reaction media (Figs. 1a, b). It was found that the aggregation/precipitation of precursor particles was suppressed at the initial reaction stage for successful growth into nanoribbon network structures, possibly because the water-soluble cellulose oligomers in the product solutions behaved as dispersion stabilizers of the precursor particles. We show a simple and

Electronic supplementary material The online version of this article (https://doi.org/10.1038/s41428-018-0057-3) contains supplementary material, which is available to authorized users.

✉ Takeshi Serizawa
serizawa@polymer.titech.ac.jp

[1] Department of Chemical Science and Engineering, School of Materials and Chemical Technology, Tokyo Institute of Technology, 2-12-1-H121 Ookayama, Meguro-ku, Tokyo 152-8550, Japan

[2] Precursory Research for Embryonic Science and Technology, Japan Science and Technology Agency, 4-1-8 Honcho, Kawaguchi-shi, Saitama 332-0012, Japan

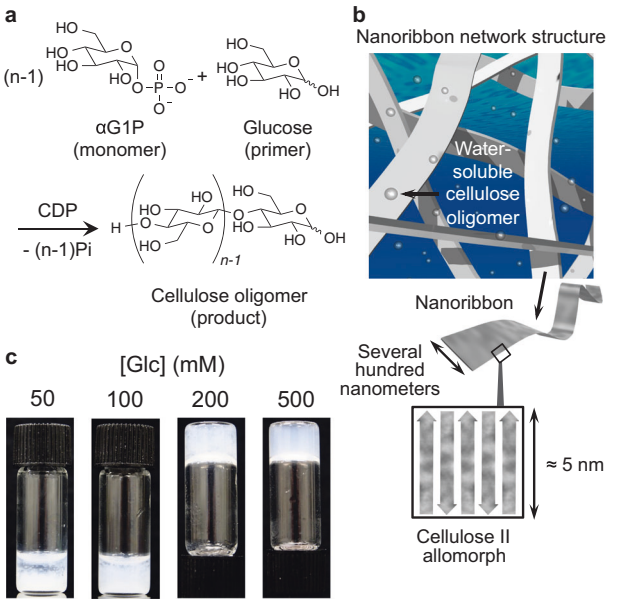

Fig. 1 **a** Reaction scheme for the CDP-catalyzed synthesis of cellulose oligomers, **b** schematic illustration of nanoribbon network structures prepared by crystallization-driven self-assembly of enzymatically synthesized cellulose oligomers at relatively high primer concentrations, and **c** photographs of the product solutions prepared at different concentrations of Glc primers

convenient production system for cellulosic hydrogels with highly grown network nanostructures using CDP-catalyzed reactions with conventional and inexpensive Glc primers.

Experimental procedures

The reaction conditions for enzymatic synthesis of cellulose oligomers using Glc primers essentially followed those reported in our previous paper [12]. In brief, αG1P monomers (200 mM) and Glc primers (50–500 mM) were incubated in 4-(2-hydroxyethyl)-1-piperazineethanesulfonic acid (HEPES) buffer solution (0.5 M, pH 7.5) containing CDP (0.2 U mL^{-1}) at 60 °C for 72 h. Unless otherwise stated, these synthetic conditions were applied throughout our experiments. The water-insoluble products were collected after washing with ultrapure water via centrifugation/redispersion cycles, except for the samples intended for scanning electron microscopy (SEM). For chemical and structural characterization, ^{1}H nuclear magnetic resonance (NMR) spectroscopy (AVANCE III HD500, Bruker Biospin, Yokohama, Japan) and matrix-assisted laser desorption/ionization time-of-flight mass spectrometry (MALDI–TOF–MS) (AXIMA Performance, Shimadzu, Kyoto, Japan) were used. For crystal structure characterizations, wide-angle X-ray diffraction (WAXD) (MiniFlex600, Rigaku Tokyo, Japan) and attenuated total reflection-Fourier transform infrared (ATR-FTIR) absorption spectrometry (FT/IR-4100, JASCO Tokyo, Japan) were used. For morphological characterization of the gelled products, SEM (JSM-7500F, JEOL Tokyo, Japan) and atomic force microscopy (AFM) (SPM-9600, Shimadzu Kyoto, Japan) were chosen. The quantification of phosphate ions eliminated from the αG1P monomers in the product solutions was in accordance with a previously reported protocol [12]. Experimental details are presented in the Supporting Information.

Results and discussion

When the concentration of Glc primers was varied in the range of 50–500 mM, the transparent reaction solutions became turbid in all cases, indicating the production of colorless and water-insoluble cellulose oligomers (Fig. 1c). Notably, above a Glc primer concentration of 200 mM, the product solutions were transformed into hydrogels, suggesting the formation of certain network structures. When the hydrogels were observed by optical microscopy as in our previous study [15], those prepared at 200 mM were macroscopically inhomogeneous, whereas those prepared at 500 mM were more homogeneous (Figure S1). This observation suggests that greater amounts of Glc primers are essential for the preparation of homogeneous hydrogels. Note that a primer concentration of 50 mM was conventional for the production of two-dimensional rectangular nanosheets as precipitates in our previous paper [12]. Therefore, this study is the first demonstration of producing hydrogels via CDP-catalyzed reactions using Glc primers. The monomer conversions estimated from the total amounts of water-insoluble products and the average DP values estimated by ^{1}H NMR measurements (see below) were found to be 35 ± 3, 39 ± 5, 38 ± 5, and 27 ± 5% at primer concentrations of 50, 100, 200, and 500 mM, respectively. Product inhibition of CDP-catalyzed reactions might be caused these moderate conversions. The monomer conversions at primer concentrations in the range of 50–200 mM were the same within experimental error and slightly decreased at a primer concentration of 500 mM. This tendency was not correlated with the gelation of the product solutions, suggesting the presence of other mechanistic reasons for gelation (the gelation mechanism is discussed later). The decrease observed at a primer concentration of 500 mM was attributed to the production of water-soluble cellulose oligomers (see below).

The chemical structures of the products were characterized. ^{1}H NMR spectra of the products revealed peaks assignable to cellulose molecules (Fig. 2a), indicating the propagation of αG1P monomers from Glc primers at all primer concentrations. The average DP values estimated

from the integral ratios for $H_{1\alpha}$ ($\delta = 5.1$), $H_{1\beta}$ ($\delta = 4.5$), and $H_{1',1''}$ ($\delta = 4.3$) protons were found to be 10, 10, 9, and 8 at primer concentrations of 50, 100, 200, and 500 mM, respectively, and tended to slightly decrease with increasing primer concentration. Furthermore, MALDI–TOF–MS of the products revealed a series of peaks assignable to the sodium and potassium ion adducts of cellulose oligomers with certain extents of DP distribution, where the peak-to-peak mass difference of 162 Da was consistent with the mass of a single glucosyl repeating unit (Fig. 2b). The average DP values estimated from the higher peak intensity for the sodium or potassium ion adducts were found to be 9, 8, 8, and 8 at primer concentrations of 50, 100, 200, and 500 mM, respectively. These values were slightly smaller than those from the ^{1}H NMR spectra, similar to a previous report [12]. Consequently, the production of cellulose oligomers via CDP-catalyzed reactions was confirmed irrespective of primer concentration.

The crystal structures of the products were characterized. WAXD profiles of the products revealed diffraction peaks at

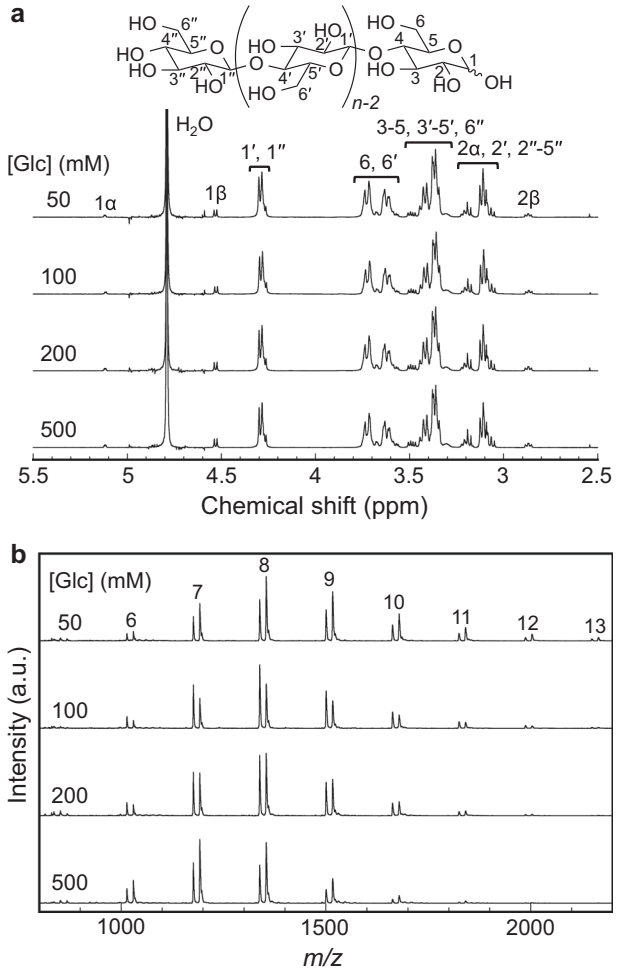

Fig. 2 **a** ^{1}H NMR spectra and **b** MALDI–TOF–MS of the products prepared at different concentrations of Glc primers

$2\theta = 12.3$, 19.9, and 22.1 degrees for *d*-spacings of 0.72, 0.45, and 0.40 nm, respectively, at all primer concentrations (Fig. 3a). These peaks are assignable to $1\bar{1}0$, 110, and 020 of the cellulose II allomorph, in which the cellulose molecules align in an antiparallel manner [11]. ATR-FTIR absorption spectra of the products also revealed peaks for vibration bands of OH stretching at 3445 and 3489 cm^{-1}, CH deformation at 1375 cm^{-1}, CH_2 scissoring at C(6) at 1418 cm^{-1}, and CH stretching at 2891 cm^{-1} of the cellulose molecules, which corresponded to the same allomorph (Fig. 3b) [17, 18]. Therefore, it was found that the crystal structures were the same for all products even though the physical states of the products (precipitate or network) were different.

The network structures of the hydrogels prepared at primer concentrations of 200 and 500 mM were morphologically characterized. SEM observations of the xerogels revealed that the hydrogels were composed of nanoribbon network structures (Fig. 4a), indicating that the cellulose oligomers synthesized at relatively high primer concentrations self-assembled into highly grown nanostructures in the product solutions. The widths and lengths were several hundred nanometers and greater than several micrometers for both primer concentrations, respectively. It seemed that branching of the nanoribbons was not produced, and therefore, the physical contact of nanoribbons was likely to cause network formation. AFM observations of the mechanically crushed nanoribbons estimated the thicknesses as 5.6 ± 0.3 and 5.3 ± 0.3 nm for primer concentrations of 200 and 500 mM, respectively (Fig. 4b). These values are comparable to the molecular length (5.2 nm) of cellodecaose (DP = 10) in the cellulose II allomorph [11]. Therefore, it was suggested that the cellulose oligomers were aligned perpendicularly to the base plane of the nanoribbons in an antiparallel manner, as schematically shown in Fig. 1b. These morphological properties are similar to those of previously reported nanoribbons composed of enzymatically synthesized cellulose oligomers [13–16].

To examine the mechanism for nanoribbon network formation, the reaction-time dependencies of the monomer conversions for all Glc primer concentrations were quantified from the total amounts of the water-insoluble products (Fig. 5a, solid line). The monomer conversions monotonically increased with reaction time in all cases, although the conversions for 500 mM Glc were slightly smaller than the others. Therefore, it was suggested that the reaction-time dependencies of the monomer conversions estimated from the water-insoluble products were not correlated with nanoribbon network formation. Furthermore, to evaluate the consumption of αG1P monomers, even for the water-soluble products with DP values normally less than 6 [19], the total amounts of phosphate ions eliminated from the

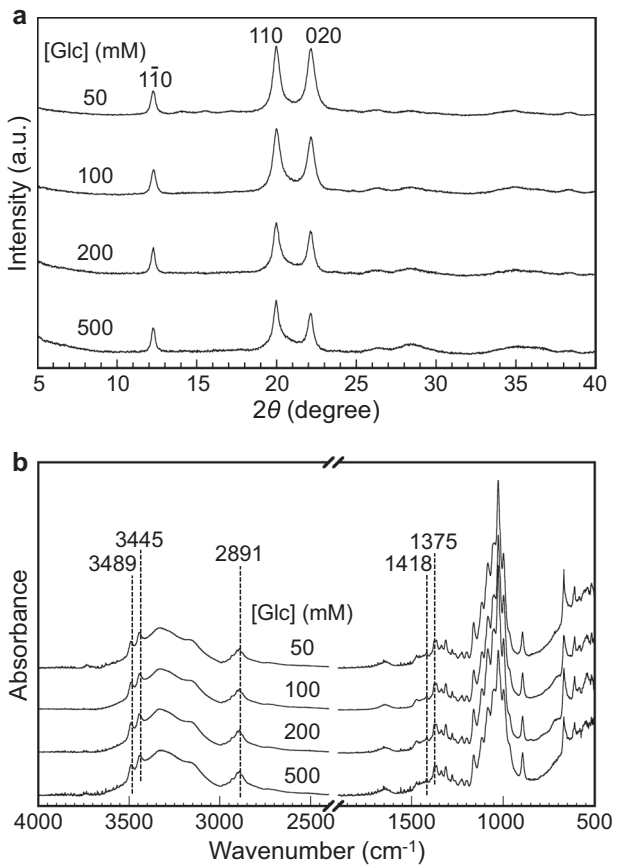

Fig. 3 **a** WAXD profiles and **b** ATR-FTIR absorption spectra of the products prepared at different concentrations of Glc primers

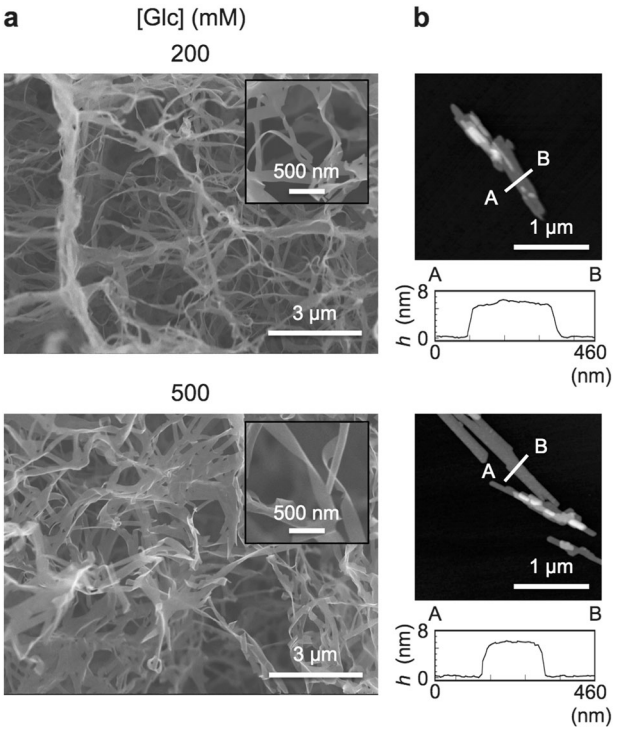

Fig. 4 **a** SEM images of the xerogels and **b** AFM images of the mechanically crushed products prepared at Glc primer concentrations of 200 and 500 mM

monomers in the product solutions were also quantified (Fig. 5a, dotted line). Both monomer conversions were similar within experimental error up to 100 mM Glc, and the conversions estimated from the phosphate ion amounts tended to be slightly greater than those determined from the water-insoluble products at concentrations above 200 mM Glc, particularly at 500 mM Glc. This observation suggested that the product solutions with concentrations above 200 mM Glc contained water-soluble cellulose oligomers. In fact, MALDI–TOF–MS revealed that the water-soluble cellulose oligomer with a DP of 6 was abundant in the supernatant of the product solution for 500 mM Glc (Figure S2). The current CDP shows the poor binding affinity for Glc primers compared with the propagated products, such as cellobiose, cellotriose, and cellotetraose [20]. Therefore, once the propagation of Glc primers is initiated, the water-soluble products are predominantly propagated until the products become water-insoluble under conventional reaction conditions using 50 mM Glc [12, 16]. At greater Glc concentrations in this study, greater amounts of Glc primers appeared to be used simultaneously to produce the water-soluble products. In our previous study on nanoribbon network formation through CDP-catalyzed synthesis of cellulose oligomers using cellobiose primers, the conversions from phosphate ions were much greater than those from the water-insoluble products [16]. The differences were attributed to kinetic control of the production of water-insoluble products for nanoribbon network formation. Because the differences in this study are much smaller than those in the previous study, kinetic control should not be predominant in this study.

However, visual aspects of the product solutions were different depending on the Glc primer concentration. Fig. 5b shows photographs of the product solutions at a reaction time of 3 h for different primer concentrations. All product solutions exist in sol states at this reaction time. The water-insoluble products were clearly observed to be precipitated or aggregated up to 100 mM Glc, whereas they were well dispersed above 200 mM Glc. This observation is acceptable when we consider that the well-dispersed precursor particles without aggregation/precipitation grow well into nanoribbon network structures in the production solutions. Note that gelation was confirmed at reaction times of approximately 12 h and 6 h at 200 mM and 500 mM Glc, respectively, indicating that the gelation time became shorter with increasing Glc primer concentration.

It is important to discuss the reason why the water-insoluble products were well dispersed at concentrations above 200 mM Glc. The aforementioned experiments indicated two results. First, large amounts of Glc primers

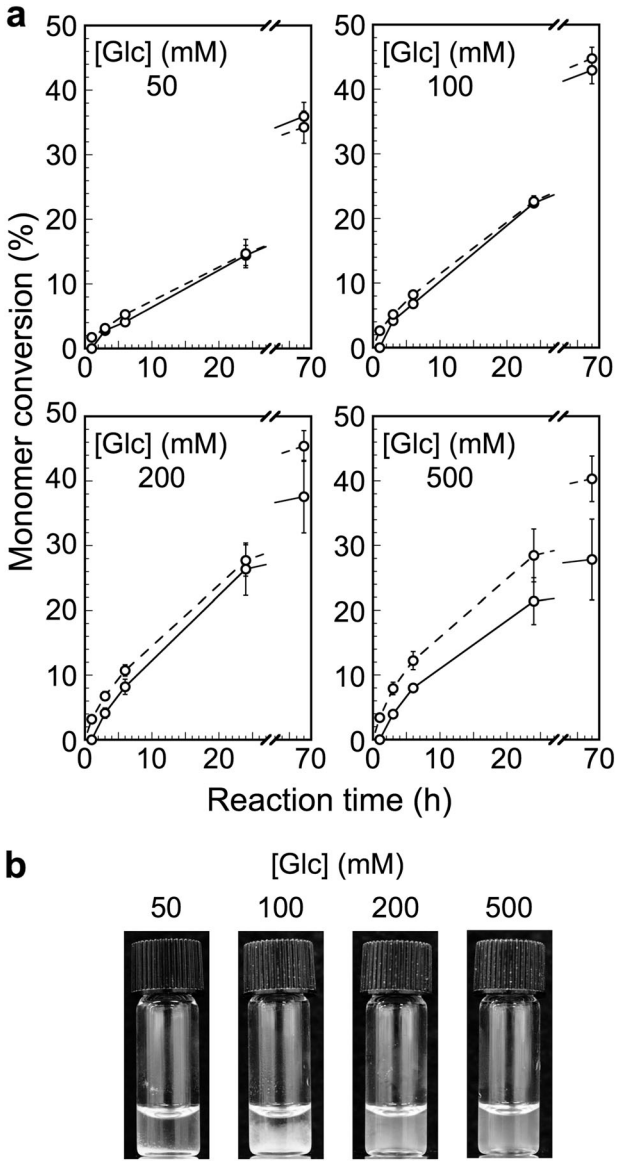

Fig. 5 **a** Reaction time-dependent monomer conversions estimated from the total amounts of water-insoluble products (solid line) or phosphate ions (dotted line) at different concentrations of Glc primers and **b** photographs of the product solutions prepared at different concentrations of Glc primers at a reaction time of 3 h

remained unreacted in the product solutions. Second, the water-soluble products were produced at concentrations above 200 mM Glc. Therefore, these molecules might act to stably disperse the water-insoluble products. To analyze the influence of the unreacted Glc primers on gelation, the CDP-catalyzed reactions were carried out at a Glc primer concentration of 50 mM in the presence of 450 mM monosaccharides such as galactose and mannose, which are not substrates for the reactions. As a result, the products were precipitated without hydrogel formation (Figure S3). Therefore, the dispersion stabilization of unreacted Glc appeared to be negated. Consequently, the water-soluble products possibly behaved as dispersion stabilizers of the precursor particles for nanoribbon network formation. Our previous studies revealed that the precursor particles were stabilized under macromolecular crowding conditions for nanoribbon network formation [14, 15]. This study newly revealed an alternative method for in situ production of nanoribbon network structures composed of the cellulose oligomers via CDP-catalyzed reactions through dispersion stabilization of precursor particles.

Conclusions

Highly grown nanoribbon network structures composed of cellulose oligomers were produced in situ by crystallization-driven self-assembly via CDP-catalyzed reverse phosphorolysis reactions using αG1P monomers and Glc primers at relatively high primer concentrations. The cellulose oligomers in the nanoribbons had average DP values of 8–9 with certain extents of DP distribution and formed the cellulose II allomorph. Morphological analyses suggested that the cellulose oligomers aligned perpendicularly to the basal plane of the nanoribbons. Analyses of reaction time dependences revealed a possible formation mechanism for the unique nanostructures in which the water-soluble cellulose oligomers possibly behaved as dispersion stabilizers of precursor particles for successful growth into nanoribbon network structures. This versatile strategy can be applied to other additives for CDP-catalyzed production of nanostructured cellulose.

Acknowledgements The authors wish to thank the Division of Materials Analysis Ookayama (Tokyo Tech) for SEM observations and WAXD measurements. This study was partially supported by the Grants-in-Aids for Scientific Research (26288056, 26620174, and 16K14075) from the Japan Society for the Promotion of Science.

Compliance with ethical standards

Conflict of interest The authors declare that they have no conflict of interest.

References

1. Klemm D, Kramer F, Moritz S, Lindström T, Ankerfors M, Gray D, Dorris A. Nanocelluloses: a new family of nature-based materials. Angew Chem Int Ed. 2011;50:5438–66.
2. Moon RJ, Martini A, Nairn J, Simonsen J, Youngblood J. Cellulose nanomaterials review: structure, properties and nanocomposites. Chem Soc Rev. 2011;40:3941–94.
3. Klemm D, Heublein B, Fink HP, Bohn A. Cellulose: fascinating biopolymer and sustainable raw material. Angew Chem Int Ed. 2005;44:3358–93.
4. Lavoine N, Desloges I, Dufresne A, Bras J. Microfibrillated cellulose – its barrier properties and spplications in cellulosic materials: a review. Carbohydr Polym. 2012;90:735–64.

5. Habibi Y, Lucia LA, Rojas OJ. Cellulose nanocrystals: chemistry, self-assembly, and applications. Chem Rev. 2010;110:3479–3500.
6. Gatenholm P, Klemm D. Bacterial nanocellulose as a renewable material for biomedical applications. MRS Bull. 2010; 35:208–13.
7. Glaser L. The sysnthesis of cellulose in cell-free extracts of acetobacter xylinum. J Biol Chem. 1958;232:627–36.
8. Kobayashi S, Kashiwa K, Kawasaki T, Shoda S. Novel method for polysaccharide synthesis using an enzyme: the first in vitro synthesis of cellulose via a nonbiosynthetic path utilizing cellulase as catalyst. J Am Chem Soc. 1991;113:3079–84.
9. Samain E, Lancelon-Pin C, Férigo F, Moreau V, Chanzy H, Heyraud A, Driguez H. Phosphorolytic synthesis of cellodextrins. Carbohydr Res. 1995;271:217–26.
10. Kadokawa J-i. Precision polysaccharide synthesis catalyzed by enzymes. Chem Rev. 2011;111:4308–45.
11. Hiraishi M, Igarashi K, Kimura S, Wada M, Kitaoka M, Samejima M. Synthesis of highly ordered cellulose II in vitro using cellodextrin phosphorylase. Carbohydr Res. 2009;344:2468–73.
12. Serizawa T, Kato M, Okura H, Sawada T, Wada M. Hydrolytic activities of artificial nanocellulose synthesized via phosphorylase-catalyzed enzymatic reactions. Polym J. 2016;48:539–44.
13. Nohara T, Sawada T, Tanaka H, Serizawa T. Enzymatic synthesis of oligo(ethylene glycol)-bearing cellulose oligomers for in situ formation of hydrogels with crystalline nanoribbon network structures. Langmuir. 2016;32:12520–6.
14. Hata Y, Kojima T, Koizumi T, Okura H, Sakai T, Sawada T, Serizawa T. Enzymatic synthesis of cellulose oligomer hydrogels composed of crystalline nanoribbon networks under macromolecular crowding conditions. ACS Macro Lett. 2017;6:165–70.
15. Hata Y, Sawada T, Serizawa T. Effect of solution viscosity on the production of nanoribbon network hydrogels composed of enzymatically synthesized cellulose oligomers under macromolecular crowding conditions. Polym J. 2017;49:575–81.
16. Serizawa T, Fukaya Y, Sawada T. Self-assembly of cellulose oligomers into nanoribbon network structures based on kinetic control of enzymatic oligomerization. Langmuir. 2017;33: 13415–22.
17. Nelson ML, O'Connor RT. Relation of certain infrared bands to cellulose crystallinity and crystal latticed type. Part I. Spectra of lattice types I, II, III and of amorphous cellulose. J Appl Polym Sci. 1964;8:1311–24.
18. Široký J, Blackburn RS, Bechtold T, Taylor J, White P. Attenuated total reflectance Fourier-transform infrared spectroscopy analysis of crystallinity changes in lyocell following continuous treatment with sodium hydroxide. Cellulose. 2010;17:103–15.
19. Zhang YH, Lynd L. Toward an aggregated understanding of enzymatic hydrolysis of cellulose: noncomplexed cellulase systems. Biotechnol Bioeng. 2004;88:797–824.
20. Krishnareddy M, Kim Y-K, Kitaoka M, Mori Y, Hayashi K. Cellodextrin phosphorylase from clostridium thermocellum YM4 strain expressed in *Escherichia coli*. J Appl Glycosci. 2002;49:1–8.